Discrete woven structure model: yarn-on-yarn friction

Bilel Ben Boubaker [a,*], Bernard Haussy [a], Jean-François Ganghoffer [b]

[a] *ESEO, 4, rue Merlet de la Boulaye, 49009 Angers cedex 01, BP 926, France*
[b] *LEMTA, UMR 7563, ENSEM, 2, avenue de la forêt de Haye, B.P. 160, 54504 Vandoeuvre cedex, France*

Abstract

A discrete model of a fabric has been developed from an analogical description, using a mass-spring system of discrete elements. An element of fabric is modeled by a set of grid nodes endowed with a mass and connected with flexional and stretching springs. This model describes the mechanical behavior of a woven structure at a mesoscopic scale. As a novel contribution, the interactions and the friction between yarns are introduced in the present work. An energy analysis of the discrete system of analogical elements is performed, taking into account the compression strain energy of the yarns and the work of the reaction forces exerted between yarns. A suitable discrete variational principle, accounting for the presence of the nonholonomic forces arising from friction, serves as a basis for a numerical implementation. Simulations of uniaxial tractions are performed, that show the effect of the yarn–yarn friction and yarn compressibility on the fabric response. *To cite this article: B. Ben Boubaker et al., C. R. Mecanique 335 (2007).*
© 2007 Académie des sciences. Published by Elsevier Masson SAS. All rights reserved.

Résumé

Modèle discret de structures tissées – Prise en compte du frottement entre fils. Un modèle discret d'une structure tissée d'armure toile a été développé, qui s'appuie sur une description analogique, mettant en œuvre un ensemble d'éléments masse-ressort. Le modèle est construit à partir d'un réseau de nœuds dotés de masses et de rigidités en rotation, connectés par des barres supposées élastiques. Le modèle décrit le comportement d'une nappe de fils à l'échelle mésoscopique. La nouveauté du présent travail réside dans la considération de la compressibilité des fils, ainsi que des interactions de frottement entre fils. Une étude énergétique du système discret est menée, en considérant l'énergie de compression des fils, ainsi que le travail des efforts de réaction exercé par les fils. Un principe variationnel discret est établi, tenant compte des forces non holonomes dues au frottement. Des simulations en traction uniaxiales mettent en évidence l'effet du frottement et de la compressibilité des fils sur la réponse du tissé. *Pour citer cet article : B. Ben Boubaker et al., C. R. Mecanique 335 (2007).*
© 2007 Académie des sciences. Published by Elsevier Masson SAS. All rights reserved.

* Corresponding author.
  E-mail addresses: Bilel.ben_boubaker@eseo.fr (B. Ben Boubaker), Bernard.haussy@eseo.fr (B. Haussy), jfgangho@ensem.inpl-nancy.fr (J.-F. Ganghoffer).

Nomenclature

$\Omega_{\text{wa}}, \Omega_{\text{we}}$ the set of warp and weft yarns, respectively

$C_{\text{ei}}, C_{\text{bi}}$ extensional and bending spring rigidity, respectively

Δ distance between two consecutive nodes

u_i, w_i extensional and vertical displacements, respectively

ψ_i rotations of the connecting nodes

$L_{\text{we}}, L_{\text{wa}}$ length of the weft and warp yarns, respectively

N_{wa} number of half-periods

$R_{\text{wa/we}}$ reaction force

L_p^{wa} half-period length

$P_{\text{wa}}, P_{\text{we}}$ traction loads applied in the x and y directions, respectively

P_{cr} beam critical compressive load

α_{we} ratio between P_{we} and $P_{\text{cr}}^{\text{we}}$

$(a_{n,k}^{\text{wa}})_{n \in [1, N_{\text{we}}]}, (a_{n,j}^{\text{we}})_{n \in [1, N_{\text{wa}}]}$ Fourier series coefficients for the warp and the weft yarns, respectively

c_k abscissa of yarn summits

$\tilde{w}_{\text{we}} = A_{\text{we}}$ amplitude of the weft yarns

$\delta_c^{\text{we}} \ and \ \delta_c^{\text{wa}}$ vertical displacements of the weft and warp under compression, respectively $C_1,$

K_1 (resp. C_2, K_2) Kawabata parameters for the warp (resp. the weft)

L_c curvilinear length of a yarn portion defined within a half-period

$w_{\text{so-we}}^j, w_{\text{so-wa}}^j$ initial displacements of weft and warp summits, respectively

$w_{\text{s-wa}}^j$ displacements of warp summits

$W_{R_{\text{we/wa}}^j}, W_{\text{reaction forces}}^k, W_{\text{traction}}, W_{\text{ext}}$ work of the reaction, traction, gravitational and external forces, respectively

N_d number of discrete elements

U_{wa}^k strain energy of the warp yarn

V_{wa}^k potential energy of the warp yarn

V potential energy

F_T friction force

α, β material constants relative to the elastic and plastic properties of the material

ℓ effective contact length between the two yarns

R radius of the considered fiber

Q_σ^{nc} generalized non-conservative forces

$\mathbf{r}_n, \mathbf{F}_T^n$ displacement and non-conservative force vectors, respectively

q_σ generalized coordinates

---

1. Introduction

Although numerous studies have been performed on the mechanical properties and behavior of woven fabric reinforced composites, less work has been spent on dry fabrics, despite their wide range of applications, see [1–4] and the references therein. The dry fabric behavior is quite peculiar, due to the ease of relative motion between yarns, which becomes prohibited when the initially dry fabric is impregnated with a resin. The relative ease of motion between yarns in turn determines the shape formed from the woven structure, and thus calls for a separate analysis [5]. As the woven structure becomes stretched, the interaction between both sets of yarns (warp and weft) is mobilized, and one should expect that the ability of the tissue to deform shall be accordingly hindered (due to a change of deformation mechanisms): it is intuitively clear that the yarn mobility is reduced at the contact zone between both yarns, specially in terms of rotation. This in turn affects the shape forming capacity of woven structures at the macroscopic scale. It is therefore important to be able to describe and quantify in an accurate manner the interactions between yarns, including friction.

A discrete model of fabric has been developed in [2,3], relying on a topological description of the yarns within a certain unit cell, in connection with given assumed kinematics of the analogical elements (extensional, flexional and torsional springs). Only the main ingredients of the model that are needed for the understanding of the subsequent developments shall be recalled here.

Few works in the literature have been devoted to the analysis of the interactions between the yarns, notwithstanding 3D finite element analysis within a context of contact mechanics [6]. From this viewpoint, the main interest of the mesoscopic approach is to incorporate the effect of the yarn interactions, without considering the three-dimensional picture inherent to a microscopic view of the yarn contact problem. For that purpose, a more refined analysis of the yarn motion is performed, whereby the yarn undulations are explicitly considered.
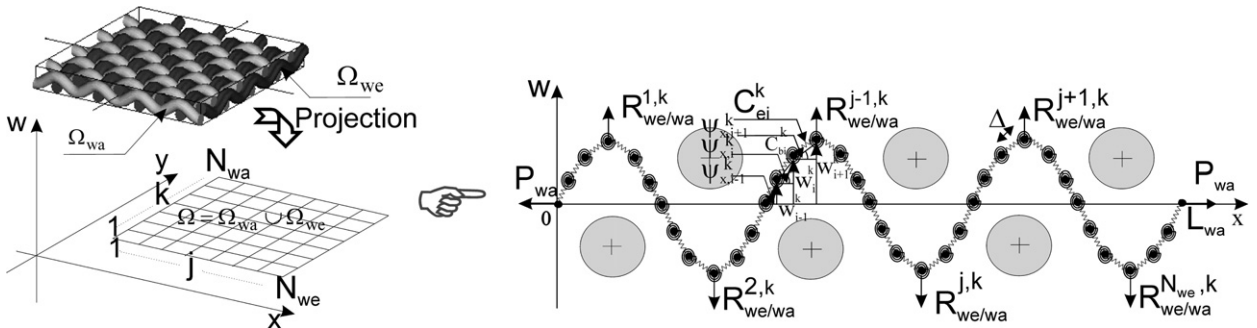
Fig. 1. Discrete model of the woven structure.

Fig. 1. Modèle discret de structures tissées.

Considering the structure as being organized into two sets of intertwined yarns Ω (the warp and the weft), the set Ω is decomposed into the assembly of two sub mechanical systems (Fig. 1), namely the set of warp yarns, Ω_{wa}, interacting with the set of weft Ω_{we}, here considered as an external (sub-mechanical) system.

The discretized yarn consists of a set of punctual masses mutually connected by extensional rigidities $C_{ei} = EA/\Delta$; each node is given a rigidity in flexion $C_{bi} = EI/\Delta$, see Fig. 1. Observe that the model takes into account dynamical aspects in the general situation, due to the presence of punctual masses. However, at least in the present applications, only a static behavior shall be considered.

The total potential energy associated to the warp yarns' system, Ω_{wa}, is first established, from a discrete description of the warp yarn shape.

2. Yarn–yarn interactions accounting for yarn compressibility

One considers in the following the plane motion of a single yarn (the warp) subjected to traction at its extremities and to the punctual contact reactions exerted by the transverse yarns (the weft), Fig. 1. The kinematics of the yarn is described on Fig. 1, and consists of the vertical displacements w_i and the rotations ψ_i of the connecting nodes. The contact forces $R_{we/wa}$ exerted by each transverse yarn are first expressed, in terms of the mechanical and geometrical yarns parameters, and the traction loads P_{wa} and P_{we} applied in the x and y directions, respectively, involving the Timoshenko beam theory [4].

At equilibrium, the deformed shapes of the fabric yarns are assumed to be periodic and expressed as the following Fourier series:

$$w_{we}^j(y) = \sum_{n=1}^{N_{wa}} a_{n,j}^{we} \sin\left((j-1)\pi + n\frac{\pi y}{L_{we}}\right); \qquad w_{wa}^k(x) = \sum_{n=1}^{N_{we}} a_{n,k}^{wa} \sin\left((k-1)\pi + n\frac{\pi x}{L_{wa}}\right)$$

for a weft yarn of index j and a warp yarn of index k respectively, where L_{wa} and L_{we} are the projected length of the warp and weft yarns, respectively on the x- and y-axes, respectively, and the $(a_{n,k}^{wa})_{n \in [1,N_{we}]}$, $(a_{n,j}^{we})_{n \in [1,N_{wa}]}$ are the Fourier series coefficients.

Using the Timoshenko's beam theory, in the case of an elastic beam subjected to an axial load P and a lateral force F exerted at a point of abscissa c, the equilibrium shape of the elastic beam is given by the Fourier development

$$w(x) = \frac{2FL^3}{\pi^4 EI} \sum_{k=1}^{N} \frac{1}{k^2(k^2 + \frac{P}{P_{cr}})} \sin\left(\frac{k\pi c}{L}\right) \sin\left(\frac{k\pi x}{L}\right) \tag{1}$$

with $P_{cr} = \pi^2 EI/L^2$, the beam critical compressive load, L the projected beam length and EI the beam bending rigidity.

Using the superposition principle, the equilibrium shape associated to a weft yarn, considered as an elastic beam which is subjected to an axial load and periodic lateral forces, is defined by

$$w_{\text{we}}^j(y) = \frac{2R_{\text{wa/we}}L_{\text{we}}^3}{\pi^4 E I_{\text{we}}} \sum_{n=1}^{N_{\text{wa}}} \sum_{m=1}^{N_{\text{wa}}/2} \frac{1}{n^2(n^2 + \alpha_{\text{we}})} \left(\sin\left(\frac{n\pi}{N_{\text{wa}}} \left(2m - \frac{3}{2} \right) \right) \right.$$

$$\left. - \sin\left(\left(2m - \frac{1}{2} \right) \frac{n\pi}{N_{\text{wa}}} \right) \right) \sin\left((j-1)\pi + \frac{n\pi y}{L_{\text{we}}} \right) \tag{2}$$

with $\alpha_{\text{we}} = P_{\text{we}}/P_{\text{cr}}^{\text{we}}$ and $P_{\text{cr}}^{\text{we}} = \pi^2 E I_{\text{we}}/L_{\text{we}}^2$. At the interlacing points of abscissa $y = c_k \ \forall k \in [1, N_{\text{wa}}]$, the double sum in (2) simplifies as

$$\left| \sum \sum \right| = \frac{1}{N_{\text{wa}}(N_{\text{wa}}^2 + \alpha_{\text{we}})} \tag{3}$$

We then deduce, from Eqs. (2), (3), the expression of the reaction forces that the warp yarns exert on the weft yarns at the interlacing points:

$$\forall y = c_k, \ \left| w_{\text{we}}(y) \right| = \tilde{w}_{\text{we}} = \frac{2R_{\text{wa/we}}}{\pi^4 E I_{\text{we}}} \frac{L_{\text{we}}^3}{N_{\text{wa}}(N_{\text{wa}}^2 + \alpha_{\text{we}})} \quad \Longleftrightarrow \quad R_{\text{wa/we}} = \frac{\pi^4}{2} \frac{E I_{\text{we}}}{(L_p^{\text{we}})^3} \left(1 + \frac{\alpha_{\text{we}}}{N_{\text{wa}}^2} \right) \tilde{w}_{\text{we}} \tag{4}$$

where $\tilde{w}_{\text{we}} = A_{\text{we}}$ is the amplitude of the weft yarns within the woven structure. This general framework shall be involved in the following to analyze the behavior of the warp yarn system Ω_{wa}, accounting for the interactions of the transverse yarns.

Under the effect of the loads P_{wa} and P_{we} applied in the warp and weft directions respectively (supposed to be uniformly distributed along the edge nodes), a lateral compressive deformation of the yarns and an undulation transfer due to the yarn–yarn interaction occur at the contact points; thus the undulation transfer process is followed by a lateral displacement of the contact points. The displacement continuity occurring at the crossing points labeled by the set of indices (j, k) then expresses as (Fig. 2(a)):

$$\delta_t^{\text{wa}} = \delta_t^{\text{we}} \quad \Rightarrow \quad w_{\text{s-we}}^{j,k} = w_{\text{so-we}}^{j,k} + w_{\text{s-wa}}^{j,k} - w_{\text{so-wa}}^{j,k} - (-1)^j \left(\delta_c^{\text{wa}} + \delta_c^{\text{we}} \right) \tag{5}$$

in which δ_c^{we} and δ_c^{wa}, respectively, denote the vertical displacement of the weft and warp under compression (Fig. 2(a)).

The deformation under compression of a warp, δ_c^{wa}, varies versus the contact force exerted by the transverse weft according to the (in inversed form) compression law of Kawabata [7], relying on measurements:

$$\delta_c^{\text{wa}} = C_1 \left(1 - e^{-K_1 |R_{\text{we/wa}}|/L_c^{\text{wa}}} \right) \quad \Longleftrightarrow \quad |R_{\text{we/wa}}| = -\frac{L_c^{\text{wa}}}{K_1} \ln\left(1 - \frac{\delta_c^{\text{wa}}}{C_1} \right) \tag{6}$$

with C_1, K_1 the two Kawabata parameters for the warp and L_c the curvilinear length of a yarn portion defined within a half-period (Fig. 2(b)).

In the same way, the deformation under compression of a weft, δ_c^{we}, varies versus the contact force exerted by the warp according to

$$\delta_c^{\text{we}} = C_2 \left(1 - e^{-K_2 |R_{\text{wa/we}}|/L_c^{\text{we}}} \right) \quad \Longleftrightarrow \quad |R_{\text{wa/we}}| = -\frac{L_c^{\text{we}}}{K_2} \ln\left(1 - \frac{\delta_c^{\text{we}}}{C_2} \right) \tag{7}$$

(a)   (b)
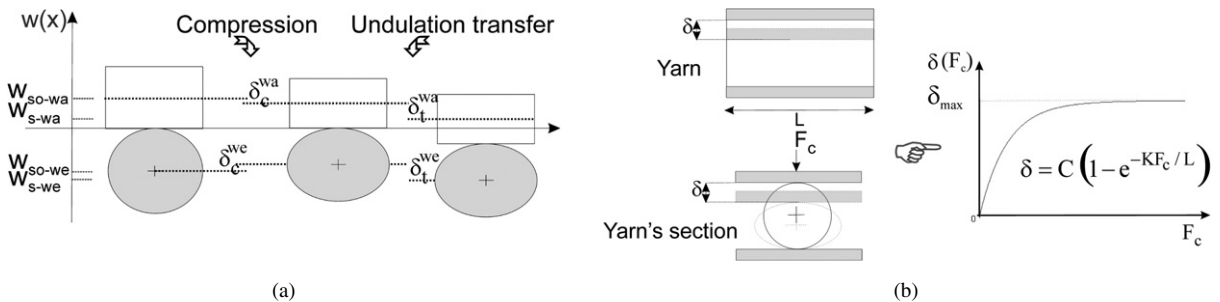
Fig. 2. (a) Compression and undulation transfer between yarns; (b) compression law for a yarn [7].

Fig. 2. (a) Compression et transfert d'ondulation entre fils ; (b) loi de compression du fil.

with C_2, K_2 the two Kawabata parameters of the weft. The parameter C can be interpreted as the limit value of the compressive deformation δ, when the compressive force increases.

The parameter K therein provides information relative to the flexibility (inversely proportional to the rigidity) of the yarn response during the compression motion. Actually, from an experimental point of view, the value of K is shown to increase as the yarn compressive rigidity decreases.

According to the action/reaction principle valid at the contact points, viz. $|R_{\text{we/wa}}| = |R_{\text{wa/we}}|$, the compression displacements of both yarns are further related by the following relationship:

$$\delta_c^{\text{we}} = C_2\left[1 - \left(1 - \frac{\delta_c^{\text{wa}}}{C_1}\right)^{\frac{K_2}{K_1}\frac{L_c^{\text{wa}}}{L_c^{\text{we}}}}\right] \tag{8}$$

From the relations (4), (5) and (8) and using the action–reaction principle, the expression of the reaction force $R_{\text{we/wa}}$ is further elaborated as

$$R_{\text{we/wa}}^{j,k} = -R_{\text{wa/we}}^{j,k} = -\frac{\pi^4}{2}\frac{(EI)_{\text{we}}}{(L_p^{\text{we}})^3}\left(1 + \frac{\alpha_{\text{we}}}{N_{\text{wa}}^2}\right)$$

$$\times \left[w_{\text{so-we}}^{j,k} + w_{\text{s-wa}}^{j,k} - w_{\text{so-wa}}^{j,k} - (-1)^j\left(\delta_{c,k}^{\text{wa}} + C_2\left[1 - \left(1 - \frac{\delta_{c,k}^{\text{wa}}}{C_1}\right)^{\frac{K_2 L_c^{\text{wa}}}{K_1 L_c^{\text{we}}}}\right]\right)\right] \tag{9}$$

The work of the reaction force $R_{\text{we/wa}}^{j,k}$, occurring at the interlacing point (j, k), then expresses as

$$W_{R_{\text{we/wa}}^{j,k}} = \int_{w_{\text{so-wa}}^{j,k}}^{w_{\text{s-wa}}^{j,k}} R_{\text{we/wa}}\, \mathrm{d}w = \int_{w_{\text{so-wa}}^{j,k}}^{w_{\text{s-wa}}^{j,k}} -\frac{\pi^4}{2}\frac{(EI)_{\text{we}}}{(L_p^{\text{we}})^3}\left(1 + \frac{\alpha_{\text{we}}}{N_{\text{wa}}^2}\right)$$

$$\times \left[(w_{\text{so-we}}^{j,k} - w_{\text{so-wa}}^{j,k}) + w - (-1)^j\left(C_2\left[1 - \left(1 - \frac{\delta_{c,k}^{\text{wa}}}{C_1}\right)^{\frac{K_2}{K_1}\frac{L_c^{\text{wa}}}{L_c^{\text{we}}}}\right] + \delta_{c,k}^{\text{wa}}\right)\right]\mathrm{d}w \tag{10}$$

Accordingly, the total work of the reaction forces exerted on a warp yarn of index k is given by

$$W_{\text{reaction forces}}^k = \sum_{j=1}^{N_{\text{we}}} W_{R_{\text{we/wa}}^{j,k}} \tag{11}$$

The previous expressions show the influence of the transversal yarns characteristics EI_{we}, L_p^{we}, $w_{\text{so-we}}$, $w_{\text{s-we}}$ and of the parameter α_{we}—which quantify the interactions between the two sub-mechanical systems Ω_{wa} and Ω_{we} during the loading—on the work of the reaction force exerted on the warp yarn.

The external work W_{ext}^k associated to the warp yarn of index k is defined by

$$W_{\text{ext}}^k = W_{\text{traction}}^k + W_{\text{gr}}^k + W_{\text{reaction forces}}^k \tag{12}$$

in which the various contributions are:

- $W_{\text{traction}}^k = P_{\text{wa}}(\sum_{i=1}^{N_d} \Delta(\cos(\psi_{x,i}^k) - \cos(\psi_{x,oi}^k)) + u_{N_d+1}^k)$—the work of the traction load P_{wa};
- $W_{\text{gr}}^k = -\sum_{i=1}^{N_d-1} m_i g(w_i^k - w_{oi}^k)$—the work of the gravity load;
- $W_{\text{reaction forces}}^k$—the work of the reaction forces at the contact points (given in (11)).

The strain energy U_{wa}^k of the same warp yarn is expressed in terms of the rotational, extensional and compressive parameters (respectively the variables $\psi_{x,i}^k$, u_i^k and δ_c^{wa}, see Fig. 1), thus giving

$$U_{\text{wa}}^k = \sum_{i=1}^{N_d-1} \frac{1}{2}C_{\text{bi}}^k\left(\psi_{x,i+1}^k - \psi_{x,i}^k\right)^2 + \sum_{i=1}^{N_d} \frac{1}{2}C_{\text{ei}}^k\left(u_{i+1}^k - u_i^k\right)^2 + \frac{L_s^{\text{wa}}}{K_1}\left[(C_1 - \delta_{c,k}^{\text{wa}})\ln\left(1 - \frac{\delta_{c,k}^{\text{wa}}}{C_1}\right) + \delta_{c,k}^{\text{wa}}\right] \tag{13}$$

representing the flexional, the extensional and the compressive deformation of the yarn successively.

The potential energy V_{wa}^k related to the warp yarn is then deduced as

$$V_{\text{wa}}^k = U_{\text{wa}}^k - W_{\text{ext}}^k \tag{14}$$

The total potential energy associated to the sub-mechanical system Ω_{wa} is finally calculated as the sum of the potential energies of all warp yarns, namely

$$V = \sum_{k=1}^{N_{\text{wa}}} V_{\text{wa}}^k \tag{15}$$

The summit index j that appears in (10) is further replaced by the global discretization index i, such that:

$$w_{\text{s-wa}}^j = w_i \quad \text{with } i = \frac{(2j-1)N_d}{2N_{\text{we}}} \text{ and } \sin(\psi_{x,i}) = \frac{w_i - w_{i-1}}{\Delta}, \ \forall i \in [1, N_d] \tag{16}$$

For small rotations, the relation (16) linking the discrete parameters $\psi_{x,i}^k$ and w_i^k can be approximated by the following expression

$$\psi_{x,i}^k \approx \left(w_i^k - w_{i-1}^k\right)/\Delta \tag{17}$$

where the discrete lateral displacements w_i^k are obtained from the discretization of the continuous shape of the k-warp yarn, given by the equation

$$w_i^k = w_{\text{wa}}^k(x_i) = \sum_{p=1}^{N_{\text{we}}} a_{p,k}^{\text{wa}} \sin\left((k-1)\pi + \frac{p\pi}{L_{\text{wa}}} x_i\right) \quad \text{with } x_i = \frac{i L_{\text{wa}}}{N_d} \tag{18}$$

Substituting Eqs. (16), (17) into expression (15), the total potential energy V becomes a function of the Fourier coefficients $(a_{p,k}^{\text{wa}})_{(p,k)\in[1...N_{\text{we}};1...N_{\text{wa}}]}$, of the yarn nodal extensions $(u_2^k, u_3^k, \ldots, u_{N_d+1}^k)_{k\in[1...N_{\text{wa}}]}$ and of the compressive parameters $(\delta_{c,k}^{\text{wa}})_{k\in[1...N_{\text{wa}}]}$ viz

$$V = V\left(a_{1,k}^{\text{wa}}, \ldots, a_{i,k}^{\text{wa}}, \ldots, a_{N_{\text{we}},k}^{\text{wa}}, u_2^k, \ldots, u_i^k, \ldots, u_{N_d+1}^k, \delta_{c,k}^{\text{wa}}\right)_{k\in[1...N_{\text{wa}}]} \tag{19}$$

To highlight the effect of yarns compressibility on the mechanical response of the fabric under uniaxial loading, traction simulations are performed in the warp direction for different values of the yarns compression rigidity (expressed by the Kawabata parameter K). The second Kawabata parameter C is supposed to keep the same constant value, for the whole set of traction tests. Since the behavior of the structure is conservative, its equilibrium shape (in terms of the set of arguments of V) is given by the minimum of its total potential energy.

For this purpose, the following input parameters are used [8]: the mechanical properties of the warp and weft yarns are taken respectively as $EI_{\text{wa}} = 1.47 \ e^{-7} \ \text{N m}$; $EI_{\text{we}} = 1.47 \ e^{-7} \ \text{N m}$; $EA_{\text{wa}} = 13.72 \ \text{N}$ and $C_1 = C_2 = 0.2 \ \text{mm}$. The rigidities in flexion/extension of the springs are then evaluated as $C_b = EI_{\text{wa}}/\Delta$ and $C_e = EA_{\text{wa}}/\Delta$, respectively. The geometrical parameters of the discretization are taken as: $L = 0.1 \ \text{m}$ (initial projected length of the set of warp); $w_{\text{so-wa}} = 0.5 \ \text{mm}$; $w_{\text{so-we}} = 0.5 \ \text{mm}$; $N_{\text{we}} = 16$ and $N_d = 224$.

Fig. 3(a) shows that a decrease of the parameter K leads to an increase of the compression rigidity, thus to a stiffer response of fabric under traction simulation. This is due to the increase of the reaction force exerted by the transversal yarns (weft yarns) (Fig 3(b)).

In fact, when the yarns compression rigidity increases, the reaction forces increase in order to prevent the undulation transfer between yarns. In addition, as shown by Eq. (10), the reaction force tends during the traction process toward a limit value, which indicates that the yarns have exhausted their possibilities of undulation transfer which means that no more lateral nodal displacement is possible. Note that the effect of yarn compression decreases with the ongoing loss of undulation (Fig. 3(a)), as a result of the saturation of the reaction force (Fig. 3(b)).

3. Incorporation of yarn–yarn friction: variational principle and numerical simulations

Several models and empirical approaches of the friction phenomena in fabric have been developed in the literature [7,9–13]. We adopt in the following, and as a matter of simplicity, the Gralen model [9,10], based on measurements for nylon and wool, and that was established in the situation of two fibers in an elastoplastic contact, being twisted,

(a)　　　　　　　　　　　　　　　　　　　　(b)
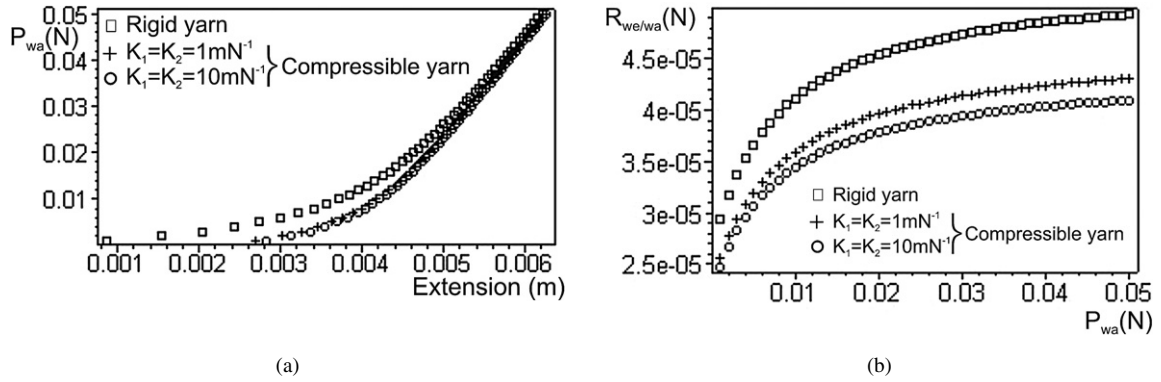
Fig. 3. (a) Uniaxial traction curve—effect of the yarns compressibility; (b) variation of the reaction force—effect of yarn compressibility.

Fig. 3. (a) Courbe de traction uniaxiale—effet de la compressibilité du fil ; (b) variation de la force de réaction—effet de la compressibilité du fil.
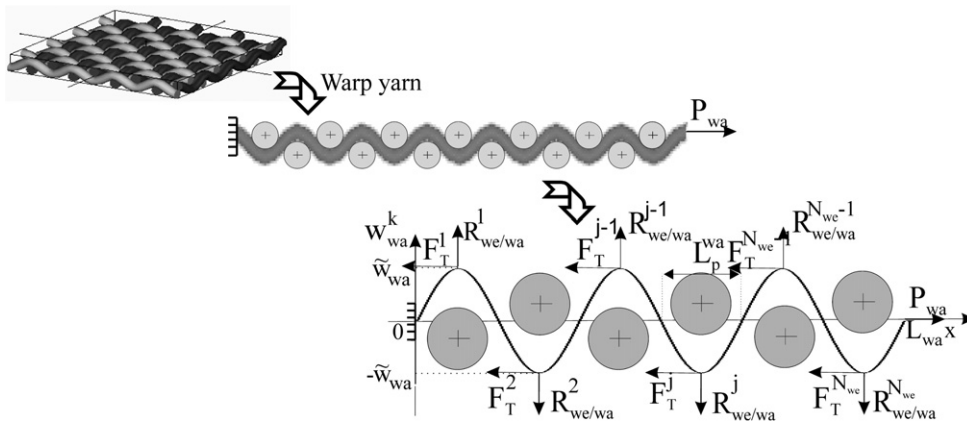
Fig. 4. Warp submitted to an external traction. Reaction and friction forces.

Fig. 4. Fil de chaîne soumis à une charge de traction. Forces de traction et de frottement.

and submitted to a compression load W. It relies on the following linear relation between the friction force and the reaction effort:

$$F_T = \alpha R_{\text{we/wa}} + \beta \ell R \tag{20}$$

with α, β two material constants relative to the elastic and plastic properties of the material, which are evaluated from measurements, ℓ the effective contact length between the two yarns, and R the radius of the considered fiber. The friction forces F_T exerted at the contact points vary versus the reaction force (normal force) exerted by the transverse yarns on the warp; a picture clarifying the yarn–yarn interactions in terms of these forces is given in Fig. 4.

Substituting next the expression (9) of the reaction force in the previous expression (20), renders

$$F_T^{j,k} = -\alpha \frac{\pi^4}{2} \frac{(EI)_{\text{we}}}{(L_p^{\text{we}})^3} \left[w_{\text{so-we}}^{j,k} + w_{\text{s-wa}}^{j,k} - w_{\text{so-wa}}^{j,k} - (-1)^j \left(\delta_{c,k}^{\text{wa}} + C_2 \left[1 - \left(1 - \frac{\delta_{c,k}^{\text{wa}}}{C_1} \right)^{\frac{K_2 L_c^{\text{wa}}}{K_1 L_c^{\text{we}}}} \right] \right) \right] + \beta \ell R \tag{21}$$

It appears from this expression that the friction forces vary not only versus the material constants, but also versus the vertical displacement of the summit nodes. During the traction process, the friction forces cause a loss of energy; this introduces an irreversible motion due to a slip of one family of yarn relative to the other one, which in turn modifies the equilibrium state of the structure. In the case of the yarn-on-yarn friction, one can remark that the friction force does not modify the previous expression of the total potential energy, given in (15); the nonholonomic forces have to be accounted for as an additional contribution on the right-hand side of the previous Euler–Lagrange equations (resulting from the stationarity of V).

A static model of friction is considered in the following. The generalization of the d'Alembert postulate of static equilibrium of motion accounting for the presence of the nonholonomic forces [14] is obtained, using the decomposition of the generalized forces $\{Q_\alpha\}_\alpha$ that intervene into the expression of the virtual work, $\delta W = \sum_{\alpha=1}^{n} Q_\alpha \delta q_\alpha$, into the sum of conservative contributions $Q_\sigma^c = -\frac{\partial V}{\partial q_\sigma}$—in which V does not depend on the rate of the generalized coordinates—and the nonholonomic forces (generalized non-conservative forces)

$$Q_\sigma^{\text{nc}} = \sum_{n=1}^{N_d} \mathbf{F}_T^n \cdot \frac{\partial \mathbf{r}_n}{\partial q_\sigma} \tag{22}$$

with $\mathbf{r}_n$ and $\mathbf{F}_T^n$ the displacement and the non-conservative force vectors of the node of index n, respectively. In (22), the generalized coordinates $(q_\sigma)_{\sigma \in \langle 1, N_{\text{we}}+N_d+1 \rangle}$ have been introduced, such that:

$$q_\sigma = \begin{cases} a_\sigma^{\text{wa}}, & \forall \sigma \in [1, N_{\text{we}}] \\ u_{\sigma-(N_{\text{we}}-1)}, & \forall \sigma \in [N_{\text{we}}+1, N_{\text{we}}+N_d] \\ \delta_c^{\text{wa}}, & \sigma = N_{\text{we}}+N_d+1 \end{cases}$$

One then obtains the differential identity

$$\frac{\partial V}{\partial q_\sigma} = Q_\sigma^{\text{nc}}, \quad \sigma \in \langle 1, N_{\text{we}}+N_d+1 \rangle \tag{23}$$

which characterizes the equilibrium shape of the yarn. The previous equation can be rewritten as

$$\frac{\partial V}{\partial q_\sigma} = Q_\sigma^{\text{nc}} = \sum_{n=1}^{N_d} \mathbf{F}_T^n \cdot \frac{\partial \mathbf{r}_n}{\partial q_\sigma}, \quad \sigma \in [1, N_{\text{we}}+N_d+1] \tag{24}$$

One obtains after projection in the Cartesian basis $(\vec{e}_x, \vec{e}_y)$:

$$Q_\sigma^{\text{nc}} = \sum_{n=1}^{N_d} \mathbf{F}_T^n \cdot \frac{\partial \mathbf{r}_n}{\partial q_\sigma} = \sum_{n=1}^{N_d} \left(-F_T^n \cdot \vec{e}_x\right) \cdot \left(\frac{\partial u_n}{\partial q_\sigma}\vec{e}_x + \frac{\partial w_n}{\partial q_\sigma}\vec{e}_y\right) = \sum_{n=1}^{N_d} -F_T^n \frac{\partial u_n}{\partial q_\sigma} \tag{25}$$

Assuming that the contact occurs only at the summit of the undulations, the friction forces are nil at other nodes, thus the previous expression simplifies to

$$Q_\sigma^{\text{nc}} = \sum_{n=1}^{N_d} -F_T^n \frac{\partial u_n}{\partial q_\sigma} = \begin{cases} \sum_{j=1}^{N_{\text{we}}} -F_T^j \frac{\partial u_j}{\partial a_\sigma^{\text{wa}}} = 0 & \text{if } \sigma \in [1, N_{\text{we}}] \\ \sum_{j=1}^{N_{\text{we}}} -F_T^j \frac{\partial u_j}{\partial u_\sigma} = \begin{cases} -F_T^j & \text{for summit nodes} \\ 0 & \text{otherwise} \end{cases} \\ \sum_{j=1}^{N_{\text{we}}} -F_T^j \frac{\partial u_j}{\partial \delta_c^{\text{wa}}} = 0 & \text{if } \sigma = N_{\text{we}}+N_d+1 \end{cases} \quad \sigma \in [1, N_{\text{we}}+N_d+1] \tag{26}$$

Accounting for the expressions (26), the equilibrium equations (23) then express as the following system of algebraic equations:

$$\begin{cases} \frac{\partial V}{\partial a_1^{\text{wa}}} = \cdots = \frac{\partial V}{\partial a_i^{\text{wa}}} = \cdots = \frac{\partial V}{\partial a_{N_{\text{we}}}^{\text{wa}}} = 0 \\ \frac{\partial V}{\partial u_i} = \begin{cases} -F_T^j & \text{if } i = \frac{(2j-1)N_d}{2N_{\text{we}}} \text{ with } j \in [1, N_{\text{we}}] \text{ (index of summit nodes)} \\ 0 & \text{otherwise} \end{cases} \\ \frac{\partial V}{\partial \delta_c^{\text{wa}}} = 0 \end{cases} \tag{27}$$
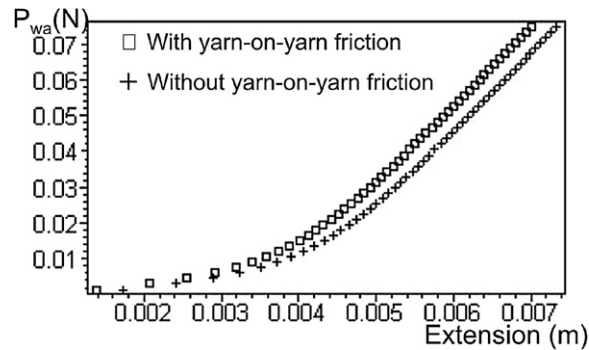
Fig. 5. Uniaxial traction curve: effect of the yarn–yarn friction.

Fig. 5. Courbe de traction uniaxiale : Effet du frottement entre fils.

The non-nil tangential displacement u_i on a summit node (Fig. 5) represents the local slip of the set of warp yarns, relative to that of the transverse weft. Note that it gives an effective representation of slip, without explicitly describing the relative slip (the nodes of both yarns are identified in the present model).

The effect of the friction on the fabric mechanical behavior is next assessed, from numerical simulations. A simulation without friction gives a reference comparison case to assess the importance of the yarn–yarn friction. For this purpose, the above mechanical parameters of the warp and weft yarns are considered. In addition, the frictional parameters of the woven structure are taken as: $\alpha = 0.2$; $\ell = 2$ mm; $R = 1$ mm and $\beta = 1\,\mathrm{e}^3\,\mathrm{N\,m}^{-2}$ [9].

Fig. 5 shows that the consideration of the yarn-on-yarn friction leads to a stiffer response. This behavior can be explained by the loss of energy due to the yarn-on-yarn friction. The importance of friction increases with ongoing extension during the first stage of deformation (up to 0.005 m), and remains thereafter constant (both curves are nearly parallel, Fig. 5), as the reaction forces increase, thus also does the friction force.

The results presented so far show that the friction and the compressibility effects are not negligible; the effect of the yarn properties on the friction behavior shall further be assessed.

Future research in this direction will take into account the effective contact area between yarns, involving a distribution of friction forces on the contact zone. Furthermore, a more accurate description of friction shall consist in a decoupling of the set of nodes where friction occurs. Suitable experiments shall then be performed in order to identify the present set of model parameters.

References

[1] M.J. King, P. Jearanaisilawong, S. Socrate, A continuum constitutive model for the mechanical behavior of woven fabrics, Int. J. Solids Structures 42 (2005) 3867–3896.

[2] B. Ben Boubaker, B. Haussy, J.F. Ganghoffer, A discrete model for the coupling between yarns in a woven fabric, C. R. Mecanique 331 (4) (2003) 295–302.

[3] B. Ben Boubaker, B. Haussy, J.F. Ganghoffer, Discrete models of fabric accounting for yarn interactions. Simulations of uniaxial and biaxial behaviour, European J. Finite Elements 14 (6–7) (2005) 653–675 (Special Issue).

[4] S. Timoshenko, Théorie de la Stabilité Elastique, Beranger, Paris & Liège, 1947.

[5] A. Gasser, P. Boisse, S. Hanklar, Mechanical behaviour of dry fabric reinforcements. 3D simulations versus biaxial tests, Comput. Mater. Sci. 17 (2000) 7–20.

[6] J. Page, J. Wang, Prediction of shear force using 3D non-linear FEM analyses for a plain weave carbon fabric in a bias extension state, Finite Elements Anal. Design 38 (8) (2002) 755–764.

[7] S. Kawabata, M. Niwa, H. Kawai, The finite deformation theory of plane weave fabrics, J. Textile Inst. 64 (1973) 21–83.

[8] SNECMA Moteurs, Le Haillan, France, Internal Report, 2002.

[9] J. Lindberg, N. Gralen, Measurement of friction between single fibers. II. Frictional properties of wool fibers measured by the fiber-twist method, Textile Res. J. (May 1948) 287–301.

[10] B. Olofsson, N. Gralen, Measurement of friction between single fibers. V. Frictional properties of viscose rayon staple fibers, Textile Res. J. 20 (7) (1950) 467–480.

[11] B.S. Gupta, Y.E. El Moghahzy, Friction in fibrous materials, Textile Res. J. 61 (9) (1991) 547–555.

[12] H.G. Howell, The laws of static friction, Textile Res. J. (1953) 589–591.

[13] H.G. Howell, J. Mazur, J. Textile Inst. 44 (1953) T59;
     B. Lincoln, British J. Appl. Phys. 3 (1952) 260.

[14] K. Arczewski, J. Pietrucha, Mathematical Modelling of Complex Mechanical Systems, vol. 1: Discrete Models, Ellis Horwood, Chichester, 1993.